

Griffiths singularity and magnetic phase diagram of $\text{La}_{1-x}\text{Ca}_x\text{CoO}_3$

Shiming Zhou*, Yuqiao Guo, Laifa He, Jiyin Zhao, and Lei Shi*
Hefei National Laboratory for Physical Science at Microscale
University of Science and Technology of China
Hefei 230026, P. R. China

August 21, 2021

*Authors to whom the correspondence should be addressed. Electronic mail: zhouism@ustc.edu.cn; shil@ustc.edu.cn

Abstract

Magnetic properties of $\text{La}_{1-x}\text{Ca}_x\text{CoO}_3$ ($0.10 \leq x \leq 0.25$) are systemically studied in this work. All the samples exhibits the ferromagnetic state at low temperatures. However, their inverse low-field magnetic susceptibilities shows a sharply downward deviation from high-temperature Curie-Weiss paramagnetic behavior well above the ferromagnetic transition temperature (T_C), which indicates the presence of a ferromagnetic clustered state above T_C . A detailed analysis on the susceptibilities reveals that the short-range state in these Ca-doped samples can be well described as the Griffiths phase. This characteristic is quite different from those of the clustered states above T_C recently reported in Sr- and Ba-doped cobaltites, which are non-Griffith-like. It is proposed that this difference possibly arises from the unique dependence of magnetic interactions among Co^{3+} ions on the size of the dopant in the doped cobaltites. Based on these results, the magnetic diagram of the Ca-doped cobaltites is established.

1 Introduction

Perovskite cobaltites $\text{La}_{1-x}\text{A}_x\text{CoO}_3$ ($A = \text{Sr}, \text{Ba}$ or Ca) have recently attracted much attention since they exhibit various intriguing physical properties such as magnetoresistance, large thermoelectric effect, insulator-metal and spin-state transitions.¹⁻⁷ The parent compound, LaCoO_3 , has a nonmagnetic insulating ground state with Co^{3+} ions in a low spin configuration. Upon warming, a paramagnetic (PM) insulating state gradually develops above ~ 90 K, where a spin-state transition from low spin (LS) to higher spin state occurs. The partial substitution of La^{3+} ions by divalent earth-alkaline ions (A) strongly affects the magnetic and transport properties of this system due to the addition of holes into

the lattice, creating formally Co^{4+} ions, and the structural changes because of the different ionic radii of the substitutes.⁸⁻¹³ A small doping can shift the spin-state transition to low temperature and rapidly suppress the nonmagnetic ground state. Consequently, ferromagnetic (FM) correlations arising from the double-exchange (DE) coupling between Co^{3+} - Co^{4+} ions appear, which develop with doping and result in a long-range FM ordered state above a critical doping level (x_C).^{8,9} Moreover, various experimental techniques such as nuclear magnetic resonance (NMR)¹⁰, small-angle neutron scattering^{11,12}, and muon spin relaxation¹³ have demonstrated that the magnetic states of doped cobaltites at low temperatures are inhomogeneous. Nanosized FM clusters were found by neutron scattering^{11,12} to form in the non-FM matrix, which increases in density with doping and coalesce at x_C . NMR measurements on the Sr-doped cobaltites revealed the coexistence of FM regions, spin-glass regions, and hole-poor LS regions at low temperatures.¹⁰

Recently, magnetic phase inhomogeneity is also found at high temperatures by the studies of small-angle neutron scattering and dc susceptibilities on $\text{La}_{1-x}\text{Sr}_x\text{CoO}_3$, where a short-range FM clustered state exists well above T_C .¹⁴ The existence of FM clusters above T_C is frequently reported in various FM oxides such as manganites,¹⁵⁻²⁰ layered cobaltites,²¹ and spin-chain compounds.²² This often leads to Griffiths singularity²³, which is originally proposed for randomly diluted Ising ferromagnets. In the original model, the nearest-neighbor exchange bonds with strength J and 0 were argued to be distributed randomly with probability p and $1 - p$, respectively. For $p < p_C$ (percolation threshold), no long-range FM order is established, while for $p \geq p_C$, the long-range FM phase exists

in a reduced $T_C(p)$ below the ordering temperature of undiluted ferromagnet $T_C(p = 1)$ known as Griffiths temperature (T_G). The region $T_C(p) < T < T_G$, where the system is characterized by the coexistence of FM clusters within the globally PM phase, is referred as the Griffiths phase. In doped perovskite FM oxides, the quenched disorder induced by the A -doping acts as random dilution. Thus, the Griffiths model can be viewed as applicable to those oxides. Actually, for various doped manganites including $\text{La}_{0.7}\text{Ca}_{0.3}\text{MnO}_3$,¹⁵ $\text{La}_{1-x}\text{Sr}_x\text{MnO}_3$ ($0.07 \leq x \leq 0.16$),¹⁶ and $\text{La}_{0.73}\text{Ba}_{0.27}\text{MnO}_3$,¹⁷ which exhibit many similarities in the magnetic and transport properties to the doped cobaltites such as hole-doping induced DE FM orderings and percolation-type insulator-metal transitions,^{3,24} the clustered phases above T_C were reported to be well described by the Griffiths phase. In those oxides, the Griffiths phase is typically characterized by a sharply downward deviation from the Curie-Weiss (CW) PM behavior in the low-field inverse susceptibility ($\chi^{-1}(T)$) as the temperature approaches T_C from above. However, for the Sr-doped cobaltites, it was found that $\chi^{-1}(T)$ exhibits an upward deviation from the high- T CW behavior, which is in stark contrast to the predictions of the Griffiths model and indicates the existence of non-Griffiths-like clustered phase in those compounds¹⁴. Similar non-Griffiths-like clustered phase was also reported in $\text{La}_{0.7}\text{Ba}_{0.3}\text{CoO}_3$.²⁵ Those results seem to point out that the FM clustered states above T_C in the doped cobaltites are quite different from those in the doped manganites. However, the clear understanding on the formation of the unique non-Griffiths-like phase is still lacking.

On the other hand, for doped cobaltites, many magnetic studies have demonstrated

that their magnetic properties strongly depend on the ionic size of the dopant.²⁶⁻²⁹ Specially, compared to the two cases doped by larger ions, i.e., $A = \text{Sr}$ or Ba , the Ca-doped crystals exhibit significant distinctions in the magnetic behaviors. For example, for $A = \text{Sr}$ and Ba , x_C is around 0.20,²⁶ while for $A = \text{Ca}$, it is reported that x_C is much lower as about 0.05.^{27,28} Furthermore, at the same doping level, T_C and the saturation moment for Ca doped ones are somewhat lower and smaller than those for $A = \text{Sr}$ and Ba , respectively.^{26,28} Recent elastic neutron scattering revealed that in crystals with Sr and Ba , Jahn-Teller (JT) spin polarons associated with intermediate-spin (IS) state Co^{3+} ions are present, whereas they are not detected in those with Ca .²⁹ Therefore, there are two interesting issues to be addressed: (1) Whether is a short-range FM state present above T_C in the Ca-doped cobaltites, similar to the Sr- and Ba-doped ones? (2) if present, whether is it a non-Griffiths-like or Griffiths-like phase? However, until now, to the best of our knowledge, no study on the magnetic inhomogeneity above T_C for the Ca-doped cobaltites is carried out.

In this work, the magnetic properties of $\text{La}_{1-x}\text{Ca}_x\text{CoO}_3$ (LCCO) ($0.10 \leq x \leq 0.25$) are systemically studied and the above issues are focused on. We find that the magnetic susceptibilities for all the Ca-doped samples deviate from the CW law well above T_C , which indicates that a short-range FM state also exists in this compound. However, quite different from the Sr- and Ba-doped cobaltites, but similar to the doped manganites, the deviation is sharply downward and the short-range FM state herein can be well viewed as the Griffiths phase. The possible origin of this important difference is discussed.

2 Experimental Section

Polycrystalline LCCO ($0.10 \leq x \leq 0.25$) were prepared by conventional solid-state reaction. The stoichiometric mixture of La_2O_3 , CaCO_3 , and Co_3O_4 powders was well ground and then calcined at 1000 and 1100 °C for 24h with intermittent grinding. The pellets pressed from the powders were sintered at 1200 °C in the flowing oxygen for 48 h. The x-ray diffraction (XRD) patterns were measured at room temperature on a Rigaku TTR-III diffractometer using $\text{Cu K}\alpha$ radiation. The magnetic measurements were carried out with a superconducting quantum interference device magnetometer (Quantum Design MPMS XL-7).

3 RESULTS AND DISCUSSION

Room temperature XRD patterns of LCCO are shown in Fig. 1. All diffraction peaks for each sample can be well indexed by the perovskite structure without any impure phases. The samples with $x \leq 0.18$ has rhombohedral symmetry, while for $x = 0.25$, it has orthorhombic symmetry. Around $x = 0.20$, there is a structural change from rhombohedral to orthorhombic symmetry, as shown in the inset of Figure 1. These results are in good agreement with the previous structural studies on the Ca-doped cobaltites.^{26,27}

Figure 2 shows the temperature dependent field-cooling (FC) magnetization under $H = 100$ Oe for LCCO. Upon cooling, the magnetization for all the samples shows a sharp rise, indicating the FM ground state at low temperature. T_C , identified from the minimum in dM/dT , increases from ~ 52 to 151 K as x increases from 0.10 to 0.25, as summarized

in Figure 5.

The temperature dependence of $\chi^{-1}(T)$ under $H = 100$ Oe for all the samples are shown in Figure 3. The susceptibilities exhibit a CW PM behavior at high temperatures, i.e. $\chi(T) = C/(T - \Theta)$, where C is Curie constant and θ is CW temperature. The fitting θ and the effective magnetic moment (μ_{eff}) obtained from the fitting C are plotted in Figure 4. Both the parameters show an increase with x . The increase in θ , together with the increase of T_C , indicates that the FM interactions are enhanced with doping. For doped cobaltites, the theoretical value of μ_{eff} is given by $\mu_{eff} = g\sqrt{(1-x)S^{3+}(S^{3+} + 1) + xS^{4+}(S^{4+} + 1)}$, where S^{3+} and S^{4+} are the spin value of Co^{3+} and Co^{4+} ions, respectively, and g is Landé g factor. Both Co ions have three possible spin states, i.e., LS, IS, and high-spin (HS) states. For Co^{3+} ions, it is widely accepted to be in IS state in doped cobaltites, while for Co^{4+} ions the spin state is more controversial.³⁰⁻³² Assuming the spin state of Co^{4+} ions are in LS, IS, and HS ones, respectively, we can calculate the theoretical μ_{eff} as a function of x , which are shown in Figure 4(a). It is clear that the IS case is most in accord with the experimental result. Therefore, both Co ions are in IS states for those Ca-doped samples in the high- T PM state.

Upon cooling, one can see that $\chi^{-1}(T)$ for LCCO shows a deviation from the CW law well above T_C , which strongly suggests that a short-range FM state exists before the long-range FM transition in those compounds. The x -dependence of T_G , i.e., the temperature below which $\chi^{-1}(T)$ starts to deviate, is plotted in Figure 5, which shows a slight increase from 161 to 181 K with doping. This result together with those recently reported in the

Sr- and Ba-doped cobaltites^{14,25} imply that the preformation of the FM clustered state above T_C should be a common phenomenon in hole-doped LaCoO₃. However, in contrast with the two cases doped by larger ions, where the deviation in $\chi^{-1}(T)$ is upward, the Ca-doped samples exhibit the sharply downward deviations in $\chi^{-1}(T)$. The downturn, similar to those reported in the doped manganites,¹⁵⁻¹⁷ is a typical characteristic of the Griffiths phase. In the Griffiths phase, the downward deviation in low-field $\chi^{-1}(T)$ is proposed to originate from the enhanced $\chi(T)$ due to the contribution from the FM clusters above T_C , and can be gradually suppressed with increasing H due to polarization of spins outside the clusters.^{14,17-19} To verify the latter feature, we have further measured the magnetizations under $H = 500$ and 5k Oe for those compounds and plotted the corresponding $\chi^{-1}(T)$ in Figure 3, too. It is clearly seen that the deviation is markedly suppressed indeed under the larger magnetic fields for all the samples, which supports the presence of the Griffiths singularity in LCCO.

According to the model of Griffiths phase, the system exhibits neither a pure PM behavior nor a long-range FM order in the Griffiths phase regime.^{17-19,23} Consequently, the system response is dominated by the largest magnetic cluster/correlated volume, which will give rise to a characteristic T -dependence for the low-field susceptibility by the following power law: $\chi^{-1}(T) \propto (T - T_C^R)^{1-\lambda}$, where λ is the susceptibility exponent and $0 < \lambda < 1$.¹⁷⁻¹⁹ In order to further confirm the Griffiths singularity in LCCO, we have fitted $\chi^{-1}(T)$ under $H = 100$ Oe by the above law for all the samples. It is pertinent to note that an incorrect value of T_C^R in this formula can lead to unphysical fitting and erroneous

determination of λ . To estimate λ accurately, we have followed the approach by Jiang et al.¹⁸, where T_C^R is correctly given as fitting the data in the pure PM region above T_G to this law yields a value of λ close to zero. In that approach, T_C^R is essentially equivalent to the value of θ . The double-logarithmic plots of χ^{-1} against reduced temperature $t_m = (T - T_C^R)/T_C^R$ for all the samples are displayed in the inset of Figure 3. From the slope of the fitted straight line in the Griffiths phase regime, the exponent λ for LCCO is obtained, which is plotted in Figure 4(c). For all the samples, the values of λ are less than unity, well consistent with the expectation from the Griffiths phase model. Moreover, it is found that the exponent λ decreases with the increase of x . Since λ signifies the deviation from the CW behavior and higher its value the stronger is the deviation,¹⁹ this decrease implies that the Griffiths phase is weakened as x increases, which well agrees with the fact that the temperature range of the Griffiths phase decreases upon doping as shown in the magnetic phase diagram of LCCO (see Figure 5). This evolution of the Griffiths phase with the composition is very similar to those reported in the doped manganite $\text{La}_{1-x}\text{Sr}_x\text{MnO}_3$ ¹⁶ and $\text{La}_{1-x}\text{Ba}_x\text{MnO}_3$ ¹⁷ and can be comparable with the $T - p$ phase diagram from the Griffiths model.^{16,17} These features strongly indicate that the clustered state in LCCO can be well described by the Griffiths phase.

Our magnetic studies unequivocally reveal that the FM clustered state above T_C in the Ca-doped cobaltites is significantly different from those reported in the Sr- and Ba-doped ones. Now, let us to discuss the possible origin of this important difference. Usually, the quenched disorder or the competition between magnetic interactions are

argued to be the fundamental ingredient in the onset of the Griffiths phase.^{17–19} For example, in $\text{La}_{1-x}\text{Ba}_x\text{MnO}_3$, the quenched disorder arising from the size variance of La/Ba atoms was reported to be responsible for the development of the Griffiths phase,¹⁷ while in $(\text{La}_{1-y}\text{Pr}_y)_{0.7}\text{Ca}_{0.3}\text{Mn}^{16/18}\text{O}_3$, a close relationship between the FM-antiferromagnetic (AFM) phase competition and the nucleation of the Griffiths phase was observed, where the Griffiths phase appears as the FM phase dominates and disappears as the AFM phase dominates over the FM one.¹⁸ Recently, we have found that a size-induced transition from non-Griffiths to Griffiths phase exists in $\text{Sm}_{0.5}\text{Sr}_{0.5}\text{MnO}_3$ nanoparticles, which is proposed due to the strong suppression of the AFM interactions above T_C by the size reduction.²⁰ For the doped cobaltites, since the samples with $A = \text{Sr}$ or Ba have a relatively larger quenched disorder because of the larger difference in the radii between La and A ions, the quenched disorder seems not the origin of the Griffiths phase in the Ca-doped samples. For the Sr- and Ba-doped ones, the observed upward deviation in $\chi^{-1}(T)$ from the CW law implies that $\chi(T)$ is reduced to be lower than the value expected from the pure PM behavior. This reduction is most probably due to the presence of AFM interactions. Alternatively, He et al. speculated that the interactions between the antiparallel alignment of neighboring FM clusters could be AFM.¹⁴ We note that in the doped cobaltites the DE coupling between Co^{3+} - Co^{4+} ions is FM, while the superexchange interactions among IS Co^{3+} ions can be AFM or FM, depending on whether the splitting of e_g orbitals, *i.e.*, JT distortion, happen or not.^{33–35} In other words, the e_g orbital ordering of Co^{3+} ions with JT distortion yields AFM spin correlations, whereas the suppression of the JT distortion

will lead the orbitals to favor FM superexchange. For $\text{La}_{1-x}\text{A}_x\text{CoO}_3$, the JT distortion is strongly dependent on the ionic size of the A-site dopant. Structural studies by the neutron diffractions have disclosed that the JT distortion associated with IS Co^{3+} ions are present in crystals with Sr and Ba but suppressed in those with Ca.^{28,29} This gives a clue to argue that the interactions between Co^{3+} ions are AFM in the crystals doped by Sr and Ba but are FM in the case by Ca. Practically, recent elastic neutron scattering on the doped cobaltites indeed revealed that the AFM ordered state is observed only for $A = \text{Sr}$ and Ba but not for $A = \text{Ca}$.³⁶ Therefore, we propose that for $A = \text{Sr}$ and Ba the presence of the AFM correlations from the Co^{3+} ions with the JT distortion results in the upward deviation in $\chi^{-1}(T)$ and hence the non-Griffiths-like phase. However, for $A = \text{Ca}$, the AFM interactions are suppressed due to the absence of the JT distortion, which promotes the appearance of the Griffiths phase.

4 Conclusions

In conclusion, the magnetic studies on $\text{La}_{1-x}\text{Ca}_x\text{CoO}_3$ reveal that the FM clustered state exists above T_C in this compound. Moreover, it is found that this state has the basic characteristics of the Griffiths phase, which is quite different from those recently reported in the Sr- and Ba-doped cobaltites where they are non-Griffiths-like. It is proposed that this difference possibly arises from the quite distinct magnetic interactions between Co^{3+} ions in those doped cobaltites. On the base of these results, we establish the magnetic diagram of the Ca-doped cobaltites.

5 Acknowledgement

This project was financially supported by the National Science Foundation of China (Grant No.10904135), the National Basic Research Program of China (973 program, 2012CB927402 and 2009CB939901), and the Foundation for the Excellent Youth Scholars of Anhui Province of China (No.2010SQRL007ZD).

References

- [1] Briceno, G.; Chang, H. Y.; Sun, X. D.; Schultz, P. G.; Xiang, X. D. *Science* **1995**, 270, 273.
- [2] Wang, Y; Sui, Y.; Ren, P.; Wang, L.; Wang, X. J.; Su, W. H.; Fan, H. J. *Inorg. Chem.* **2010**, 49, 3216.
- [3] Aarbogh, H. M.; Wu, J.; Wang, L.; Zheng, H.; Mitchell, J. F.; Leighton, C. *Phys. Rev. B* **2006**, 74, 134408.
- [4] Tong, P.; Yu, J.; Huang, Q.; Yamada, K.; Louca, D. *Phys. Rev. Lett.* **2011** 106, 156407.
- [5] Radaelli, P. G.; Cheong, S. W. *Phys. Rev. B* **2002**, 66, 094408.
- [6] Podlesnyak, A.; Streule, S.; Mesot, J.; Medarde, M.; Pomjakushina, E.; Conder, K.; Tanaka, A.; Haverkort, M. W.; Khomskii, D. I. *Phys. Rev. Lett.* **2006**, 97, 247208

- [7] Klie, R. F.; Zheng, J. C.; Zhu, Y.; Varela, M.; Wu, J.; Leighton, C. *Phys. Rev. Lett.* **2007**, 99, 047203.
- [8] Podlesnyak, A.; Russina, M.; Furrer, A.; Alfonsov, A.; Vavilova, E.; Kataev, V.; Büchner, B.; Strässle, T.; Pomjakushina, E.; Conder, K.; Khomskii, D. I. *Phys. Rev. Lett.* **2008**, 101, 247603.
- [9] Podlesnyak, A.; Ehlers, G.; Frontzek, M.; Sefat, A. S.; Furrer, A.; Strässle, T.; Pomjakushina, E.; Conder, K.; Demmel, F.; Khomskii, D. I. *Phys. Rev. B* **2011**, 83, 134430.
- [10] Kuhns, P. L.; Hoch, M. J. R.; Moulton, W. G.; Reyes, A. P.; Wu, J.; Leighton, C. *Phys. Rev. Lett.* **2003**, 91, 127202.
- [11] Caciuffo, R.; Rinaldi, D.; Barucca, G.; Mira, J.; Rivas, J.; Senaris-Rodriguez, M. A.; Radaelli, P. G.; Fiorani, D.; Goodenough, J. B. *Phys. Rev. B* **1999**, 59, 1068.
- [12] Wu, J.; Lynn, J. W.; Glinka, C. J.; Burley, J.; Zheng, H.; Mitchell, J. F.; Leighton, C. *Phys. Rev. Lett.* **2005**, 94, 037201.
- [13] Giblin, S. R.; Terry, I.; Prabhakaran, D.; Boothroyd, A. T.; Wu, J.; Leighton, C. *Phys. Rev. B* **2006**, 74, 104411.
- [14] He, C.; Torija, M. A.; Wu, J.; Lynn, J. W.; Zheng, H.; Mitchell, J. F.; Leighton, C. *Phys. Rev. B* **2007**, 76, 014401.
- [15] Salamon, M. B.; Lin, P.; Chun, S. H. *Phys. Rev. Lett.* **2002**, 88, 197203.

- [16] Deisenhofer, J.; Braak, D.; Krug von Nidda, H.-A.; Hemberger, J.; Eremina, R. M.; Ivanshin, V. A.; Balbashov, A. M.; Jug, G.; Loidl, A.; Kimura, T.; Tokura, Y. *Phys. Rev. Lett.* **2005**, 95, 257202.
- [17] Jiang, W. J.; Zhou, X. Z.; Williams, G.; Mukovskii, Y.; Glazyrin, K. *Phys. Rev. B* **2008**, 77, 064424.
- [18] Jiang, W. J.; Zhou, X. Z.; Williams, G. *Europhys. Lett.* **2008**, 84, 47009.
- [19] Pramanik, A. K.; Banerjee, A. *Phys. Rev. B* **2010**, 81, 024431.
- [20] Zhou, S. M.; Guo, Y. Q.; Zhao, J. Y.; He, L. F.; Shi, L. *J. Phys. Chem. C* **2011**, 115, 1535.
- [21] Shimada, Y.; Miyasaka, S.; Kumai, R.; Tokura, Y. *Phys. Rev. B* **2006**, 73, 134424.
- [22] Sampathkumaran, E. V.; Mohapatra, N.; Rayaprol, S.; Iyer, K. K. *Phys. Rev. B* **2007**, 75, 052412.
- [23] Griffiths, R. B. *Phys. Rev. Lett.* **1969**, 23, 17.
- [24] Hoch, M. J. R.; Kuhns, P. L.; Moulton, W. G.; Reyes, A. P.; Torija, M. A.; Mitchell, J. F.; Leighton, C. *Phys. Rev. B* **2007**, 75, 104421.
- [25] Huang, W. G.; Zhang, X. Q.; Li, G. K.; Sun, Y.; Li, Q. A.; Cheng, Z. H. *Chinese Physics B* **2009**, 18, 1674.

- [26] Kriener, M.; Zobel, C.; Reichl, A.; Baier, J.; Cwik, M.; Berggold, K.; Kierspel, H.; Zabara, O.; Freimuth, A.; Lorenz, T. *Phys. Rev. B* **2004**, 69, 094417.
- [27] Kriener, M.; Braden, M.; Kierspel, H.; Senff, D.; Zabara, O.; Zobel, C.; Lorenz, T. *Phys. Rev. B* **2009**, 79, 224104.
- [28] Phelan, D.; Louca, D.; Kamazawa, K.; Hundley, M. F.; Yamada, K. *Phys. Rev. B* **2007**, 76, 104111.
- [29] Phelan, D.; Yu, J.; Louca, D. *Phys. Rev. B* **2008**, 78, 094108.
- [30] Wu, J.; Leighton, C. *Phys. Rev. B* **2003**, 67, 174408.
- [31] Burley, J. C.; Mitchell, J. F.; Short, S. *Phys. Rev. B* **2004**, 69, 054401.
- [32] Tsubouchi, S.; Kyômen, T.; Itoh, M.; Oguni, M. *Phys. Rev. B* **2004**, 69, 144406.
- [33] Fuchs, D.; Pinta, C.; Schwarz, T.; Schweiss, P.; Nagel, P.; Schuppler, S.; Schneider, R.; Merz, M.; Roth, G.; Löhneysen, H. *Phys. Rev. B* **2007**, 75, 144402.
- [34] Zhou, S. M.; Shi, L.; Zhao, J. Y.; He, L. F.; Yang, H. P.; Zhang, S. M. *Phys. Rev. B* **2007**, 76, 172407.
- [35] Zhou, S. M.; He, L. F.; Zhao, S. Y.; Guo, Y. Q.; Zhao, J. Y.; Shi, L. *J. Phys. Chem. C* **2009**, 113, 13522.
- [36] Yu, J.; Louca, D.; Phelan, D.; Tomiyasu, K.; Horigane, K.; Yamada, K. *Phys. Rev. B* **2009**, 80, 052402.

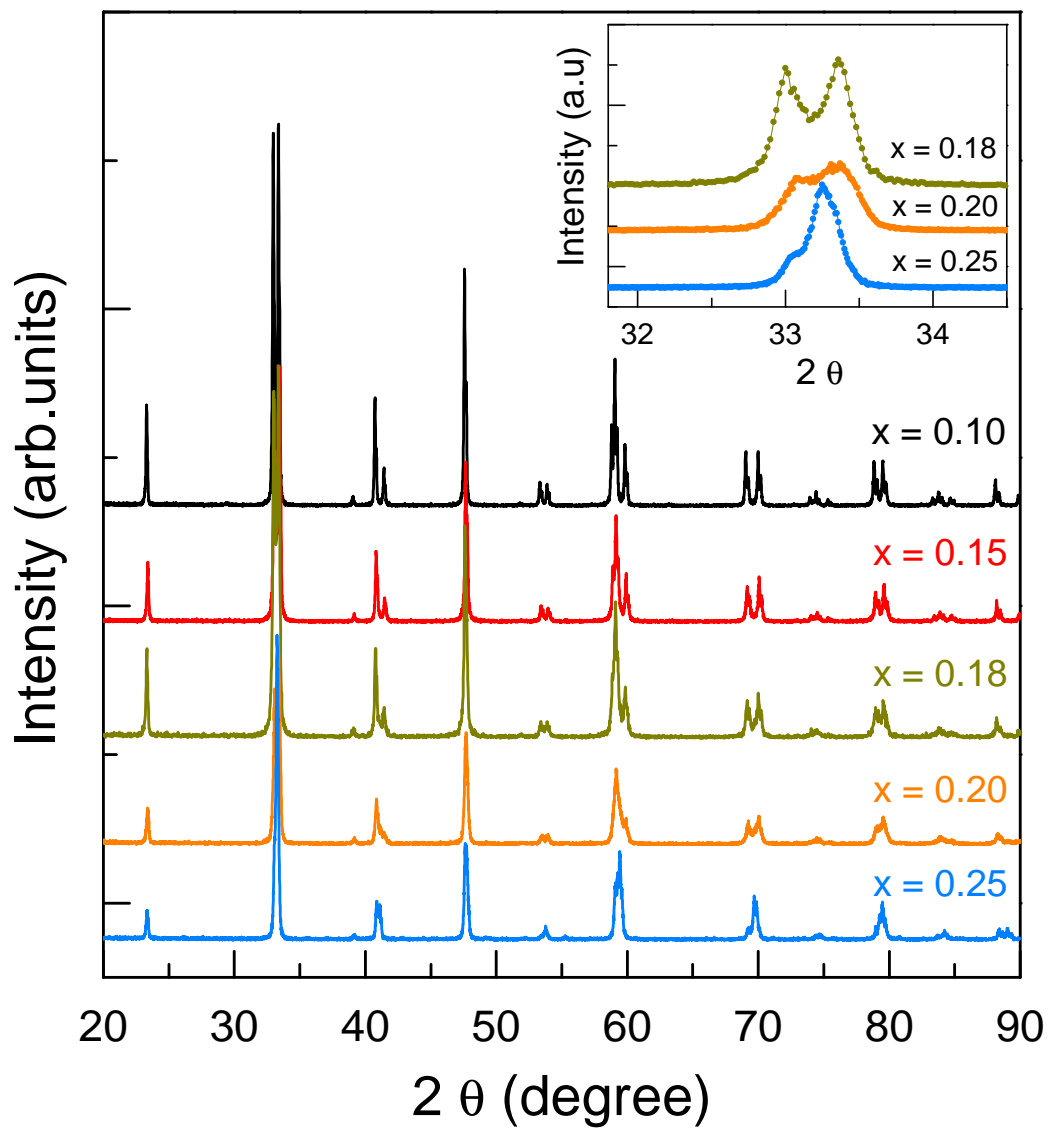
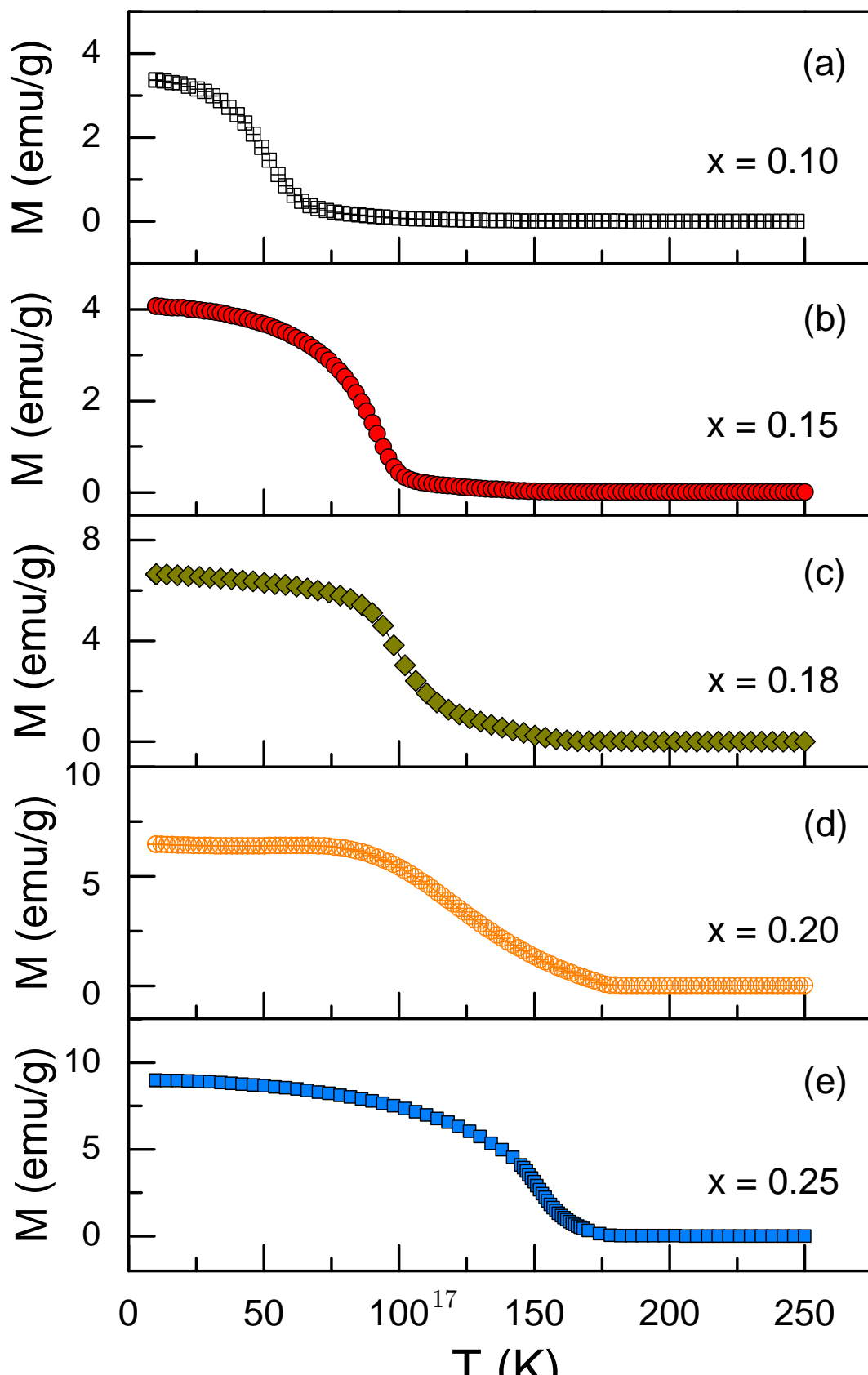


Figure 1: (Color online) Room-temperature XRD patterns for $\text{La}_{1-x}\text{Ca}_x\text{CoO}_3$ ($0.10 \leq x \leq 0.25$). The insets shows the structural change around $x = 0.20$.



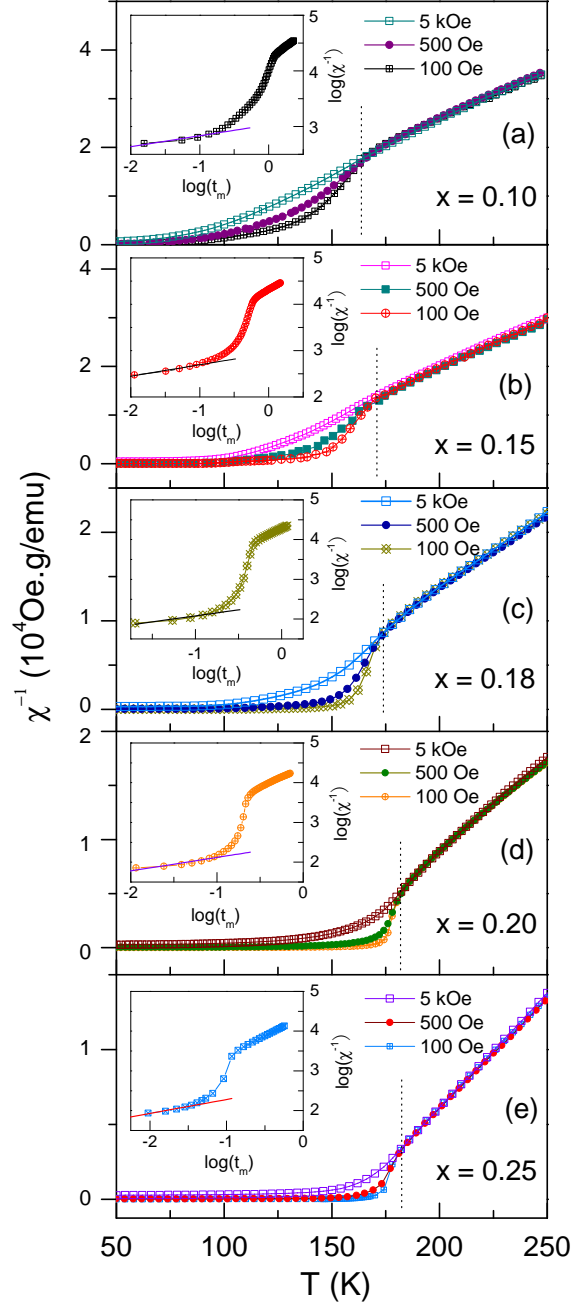
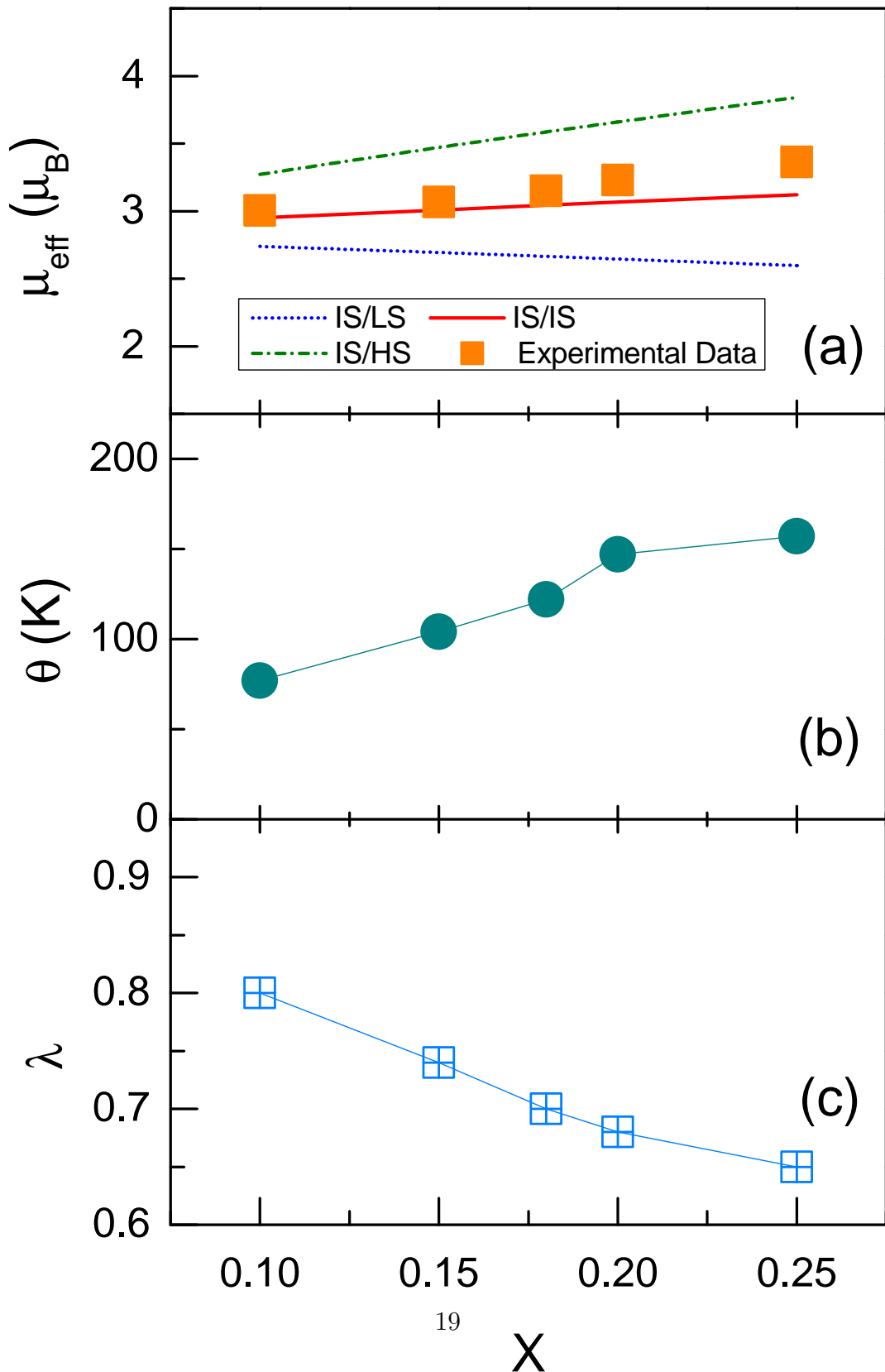


Figure 3: (Color online) Temperature dependence of the inverse susceptibilities under different magnetic fields for $\text{La}_{1-x}\text{Ca}_x\text{CoO}_3$ ($0.10 \leq x \leq 0.25$). The insets show $\log(\chi^{-1}(T))$ vs $\log(t_m)$ plots under $H = 100$ Oe, where the solid lines are the linear fittings.



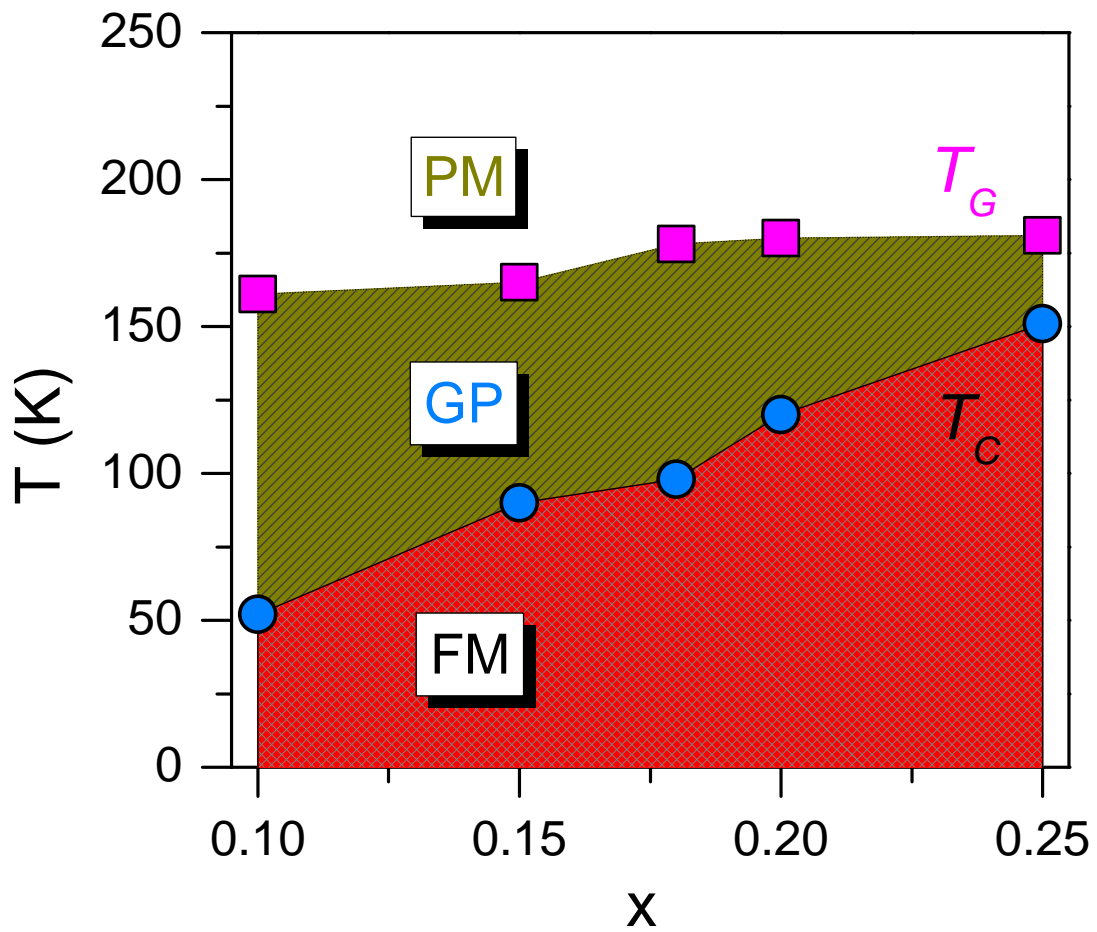


Figure 5: (Color online) Magnetic phase diagram of $\text{La}_{1-x}\text{Ca}_x\text{CoO}_3$ ($0.10 \leq x \leq 0.25$). PM, GP, and FM denote the paramagnetic, Griffiths, and ferromagnetic phase, respectively.